Photovoltaic mismatch losses caused by moving clouds

Solar Energy 158 (2017) 455–461

Contents lists available at ScienceDirect

Solar Energy

journal homepage: www.elsevier.com/locate/solener

Photovoltaic mismatch losses caused by moving clouds

Kari Lappalainen*, Seppo Valkealahti

Tampere University of Technology, Laboratory of Electrical Energy Engineering, P.O. Box, 692, FI-33101 Tampere, Finland

ARTICLE INFO

Keywords:
Photovoltaic power generation
Mismatch losses
Partial shading
Irradiance transition

ABSTRACT

Mismatch losses is a major issue in the photovoltaic (PV) system and are mainly caused by partial shading; largest mismatch losses are caused by sharp shadows. These shadows are a typical problem for rooftop and residential installations. In large-scale PV plants, partial shading is mostly caused by moving clouds which produce gentle irradiance transitions causing typically only minor irradiance differences between adjacent PV modules.

This paper presents a study of the mismatch losses of PV arrays with various layouts and electrical configurations during around 27,000 irradiance transitions identified in measured irradiance data. The overall effect of the mismatch losses caused by moving clouds on the energy production of PV plants was also studied. The study was conducted using a mathematical model of irradiance transitions and an experimentally verified MATLAB/Simulink model of a PV module.

The relative mismatch losses during the identified irradiance transitions ranged from 1.4% to 4.0% depending on the electrical configuration and layout of the PV array. The overall effect of the mismatch losses caused by moving clouds on the total electricity production of PV arrays was about 0.5% for the PV array with strings of 28 PV modules and substantially smaller for arrays with shorter strings. The proportions of the total mismatch losses caused by very dark or highly transparent clouds were small. About 70% of the total mismatch losses were caused by shadow edges with shading strengths ranging between 40% and 80%. These results indicate that the mismatch losses caused by moving clouds are not a major problem for large-scale PV plants. An interesting finding from a practical point of view is that the mismatch losses increase the rate of power fluctuations compared to the rate of irradiance fluctuations.

1. Introduction

Overpassing cloud shadows are a significant reason for the mismatch losses of large-scale photovoltaic (PV) power plants. Mismatch losses are the difference between the sum of the maximum powers of individual PV cells or modules of a PV system, as if they were operating separately, and the maximum power of the whole PV system. Mismatch losses occur in every PV system when interconnected PV cells have different electrical characteristics at a specific instant. Mismatch losses are mainly caused by partial shading (PS), but they are also caused by other differences in the operation conditions of PV modules, module damages and manufacturing tolerances. PS caused by moving clouds can also lead to failures in maximum power point (MPP) tracking thereby causing additional losses. Moreover, fast irradiance transitions caused by the edges of clouds can lead to fluctuations in the output power of PV systems. While the PS of large-scale PV plants is mainly caused by overpassing cloud shadows, it can also exist due to surrounding objects, snow or soiling.

Solar radiation variability and irradiance transitions caused by the edges of moving cloud shadows have been studied in several papers, e.g. in Lappalainen and Valkealahti (2015, 2016b), Lave et al. (2015), Perez et al. (2011), Tomson (2010) and Tomson and Tamm (2006). In Lappalainen and Valkealahti (2016b), a comprehensive study of the apparent velocity of shadow edges, i.e., the component of shadow velocity normal to the shadow edge, caused by moving clouds has been presented. The apparent speed of the shadow edges has been found to vary considerably and have an average value of around 9 m/s. The length of irradiance transitions on the edges of cloud shadows has also been found to vary considerably with an average of around 150 m. When a cloud shadow is covering a PV array, the apparent speed of the shadow edge defines how rapidly the PV array is becoming shaded. Thus, the apparent velocity of a linear shadow edge is a vital quantity in any analysis of the effects of overpassing cloud shadows on the operation of small PV systems and the PV arrays of large PV power plants. Still, the assumption of linearity for the shadow edge might not be valid for large PV systems as a whole (Lappalainen and Valkealahti, 2016b).

* Corresponding author.
E-mail addresses: kari.lappalainen@tut.fi (K. Lappalainen), seppo.valkealahti@tut.fi (S. Valkealahti).

http://dx.doi.org/10.1016/j.solener.2017.10.001
Received 23 February 2017; Received in revised form 8 August 2017; Accepted 2 October 2017

The mismatch losses of PV generators caused by PS and their mitigation have been studied and reported on in several papers, especially during the past years, e.g. in Picault et al. (2010), Potnuru et al. (2015), Rakesh and Madhavaram (2016), Shams El-Dein et al. (2013a, 2013b), Vijayalekshmy et al. (2016) and Villa et al. (2012). However, these studies are based on static and hypothetical PS conditions and lack the knowledge of real irradiance transitions caused, for example, by moving clouds. Moreover, in these papers, mismatch losses caused by shadings with large irradiance differences between adjacent PV modules, i.e., extremely sharp shadows, have been studied. Mismatch losses under PS conditions caused by moving clouds have been studied using irradiance measurements in Lappalainen and Valkealahti (2017a, 2017b) and Torres Lobera and Valkealahti (2013) and electrical measurements in Rodrigo et al. (2016). Mismatch losses caused by manufacturing tolerances have been studied e.g. in Lorente et al. (2014).

The large lengths of irradiance transitions reported in Lappalainen and Valkealahti (2016b) mean that the shadows of moving clouds cause gentle irradiance transitions, leading typically only minor irradiance differences between adjacent PV modules. The result has been presented in Lappalainen and Valkealahti (2017a) that the mismatch losses of PV arrays decrease with decreasing shadow sharpness. Moreover, the differences between various electrical PV array configurations have been found to decrease with decreasing shadow sharpness. In large-scale PV plants, shading is mostly caused by moving clouds and sharp shadows, which are caused by nearby objects, can be considered as rare worst-case scenarios. In Lappalainen and Valkealahti (2017b) the mismatch losses caused by moving clouds have been estimated to be clearly below 1.0% of the total electricity production of PV arrays. However, a comprehensive study of the total mismatch losses of PV plants caused by moving clouds has not been presented as yet.

In this paper, the mismatch losses of series-parallel (SP), total-cross-tied (TCT) and multi-string (MS) electrical PV array configurations were studied during about 27,000 irradiance transitions identified in measured irradiance data. Moreover, the overall effect of the mismatch losses caused by moving clouds on the energy production of PV plants was determined based on the studied mismatch losses and irradiance measurements. The study was conducted using a mathematical model of irradiance transitions and an experimentally verified MATLAB/Simulink model of a PV module based on the well-known one-diode model of a PV cell. The presented study is based on measurements at a particular location although the characteristics of irradiance transitions may differ regionally. However, the results of this study do provide generally applicable information on the magnitude, range and total amount of the mismatch losses of various PV array layouts and electrical configurations caused by moving clouds. The results of this study are relevant, particularly from the PV array and system design point of view when aiming towards higher overall PV system efficiencies.

2. Methods and data

2.1. Simulation model for the PV modules

The PV modules were modelled by an experimentally verified MATLAB/Simulink model that is based on the model presented by Villalva et al. (2009). This model is based on the well-known one-diode model that provides the following relationship between the current and the voltage of a PV cell:

$$I = I_{ph} - I_o\left(e^{\frac{U+R_sI}{AU_T}} - 1\right) - \frac{U + R_sI}{R_{sh}}, \quad (1)$$

where I is the current, I_{ph} the light-generated current, I_o the dark saturation current, U the voltage, R_s the series resistance, A the ideality factor, U_T the thermal voltage and R_{sh} the shunt resistance of the PV cell (Wenham et al., 2007). The thermal voltage of a PV cell can be written as $U_T = kT/q$, where k is the Boltzmann constant, T the temperature of the cell and q the elementary charge. The simulation model for a PV module was obtained by scaling the parameter values used in the model of a PV cell by the number of PV cells in the PV module. Bypass diodes of the PV module were modelled using Eq. (1) by assuming that the light-generated current I_{ph} is zero and the shunt resistance R_{sh} is infinite. The dark saturation current $I_{o,\,bypass}$, the series resistance $R_{s,\,bypass}$ and the ideality factor A_{bypass} of the bypass diodes were determined by using curve fitting to a measured I–U curve of a Schottky diode. The temperature of the bypass diodes was assumed to be constant and the same as the temperature of the PV module.

Table 1
The electrical characteristics of the NAPS NP190GKg PV module for short-circuit (SC), open-circuit (OC) and MPP in STC.

Parameter	Value
$I_{SC,\,STC}$	8.02 A
$U_{OC,\,STC}$	33.1 V
$P_{MPP,\,STC}$	190 W
$I_{MPP,\,STC}$	7.33 A
$U_{MPP,\,STC}$	25.9 V

The characteristics of the PV module simulation model were fitted to the characteristics of the NAPS NP190GKg PV module used in the solar PV power station research plant of Tampere University of Technology (TUT) (Torres Lobera et al., 2013). The module is composed of 54 series-connected polycrystalline silicon PV cells and three bypass diodes, each connected in anti-parallel with 18 PV cells. The electrical characteristics of the module, given by the manufacturer, in standard test conditions (STC) are presented in Table 1. The simulation model parameter values for the PV modules and the bypass diodes are presented in Table 2. The results of the simulations could slightly change if different PV modules were used as a reference. However, the basic behavior would not change because the electrical characteristics of crystalline silicon PV modules do not differ essentially. Although the used simulation model contains simplifications and assumptions, it is accurate enough for the analysis of mismatch losses presented in this paper.

2.2. PV array configurations

The electrical connections for the studied SP, TCT and MS PV array configurations are presented in Fig. 1. These configurations were selected since SP and MS are commonly applied in PV array installations, whereas TCT is frequently reported to improve PV array performance under partially shaded conditions when compared to SP (Picault et al., 2010; Rakesh and Madhavaram, 2016; Villa et al., 2012). In the studied configurations, the series-connected PV modules were placed in straight strings of equal length to form a rectangle. The distance between the adjacent strings was 2.0 m, and there were no gaps between the series-connected modules. The east-west orientation of the PV arrays was used in the simulations, i.e., the PV strings were placed from east to west. The PV modules were mounted at a tilt angle of 45° from the horizontal

Table 2
The parameter values of the simulation model for the NAPS NP190GKg PV module and the bypass diodes.

Parameter	Value
A	1.30
R_s	0.329 Ω
R_{sh}	188 Ω
A_{bypass}	1.50
$R_{s,\,bypass}$	0.02 Ω
$I_{o,\,bypass}$	3.20 μA

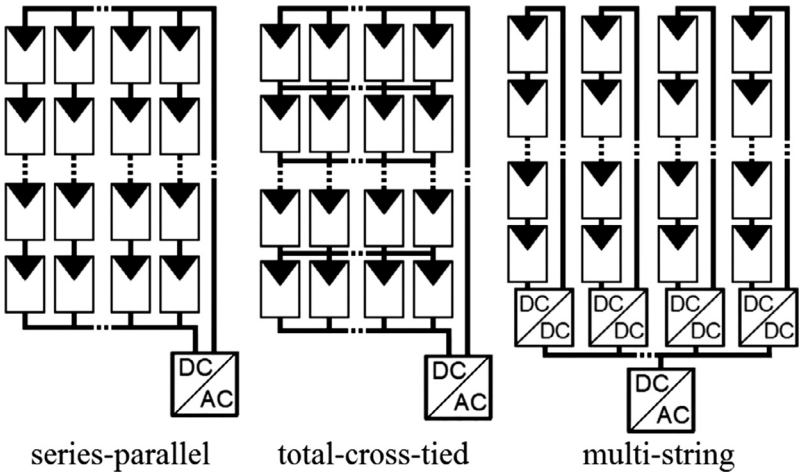

Fig. 1. The electrical connections for the studied PV array configurations.

plane.

The total number of PV modules was constant 168 for all the studied PV array layouts. The array size was restricted by the need for a reasonable computing time. The longest string selected for the study was 28 modules since that string is close to a typical string length in the PV arrays that are feeding inverters in utility-scale PV power plants. The results achieved for these array sizes are also largely valid for larger PV power plants as well since PV arrays are the operational units of large PV power plants. The nominal power of the studied PV arrays under STC was 31.92 kWp. The studied array layouts and their dimensions, calculated using the dimensions of the NAPS NP190GKg PV modules, are presented in Table 3.

2.3. Irradiance transitions and the shading of a PV array

Irradiance transitions caused by the edges of moving cloud shadows were modelled using the mathematical model offered by Lappalainen and Valkealahti (2015)

$$G(t) = \frac{G_{us} - G_s}{1 + e^{(t-t_0)/b}} + G_s, \quad (2)$$

where G is the irradiance, t the time, G_{us} the irradiance of an unshaded situation and G_s the irradiance under full shading. Parameter b is related to the steepness of the transition and its sign defines whether the transition is a fall or a rise, i.e., a decreasing or increasing transition. Parameter t_0 adjusts the transition time thereby defining the midpoint of the transition. The operation of the model has been validated with around 40,000 irradiance transitions identified in measured data by Lappalainen and Valkealahti (2015). The average root-mean-square deviation between the curve fits and the measured transitions was around 12 W/m^2. The shading strength (SS), i.e., the attenuation of irradiance due to shading, of an irradiance transition can be expressed as

$$SS = \frac{G_{us} - G_s}{G_{us}}. \quad (3)$$

By utilising Eq. (2), irradiance transitions can be defined using four variables: SS, parameter b and apparent speed and direction of movement, which have no correlation with each other (Lappalainen and Valkealahti, 2016a, 2016b). The duration of a transition was calculated by multiplying b by the experimentally obtained regression coefficient of 7.67 (Lappalainen and Valkealahti, 2016a), and the parameter t_0 was then calculated from the duration.

Table 3
The numbers of modules and the dimensions of the studied PV array layouts.

Number of modules (parallel × series)	Dimensions (m)
6 × 28	14.2 × 41.3
8 × 21	19.6 × 31.0
12 × 14	30.4 × 20.7

In this study, a total of 27,210 irradiance transitions, consisting of 13,241 falls and 13,969 rises, were exploited. The irradiance transitions were identified in 15 months (457 days) of data, measured by the irradiance sensors S2, S5 and S6 (see Torres Lobera et al. (2013)) of the TUT solar PV power station research plant located in Tampere, Finland, using the method presented by Lappalainen and Valkealahti (2015). The sensors were photodiode-based SP Lite2 pyranometers (Kipp & Zonen) mounted at a tilt angle of 45° from the horizontal plane and oriented nearly due south.

The apparent velocities of the identified shadow edges were calculated using the time lags between the shading of the three irradiance sensors using the method presented by Lappalainen and Valkealahti (2016b). The average values of the SS, the absolute value of b and the apparent speed of the identified irradiance transitions were 59.2%, 1.98 s and 8.57 m/s, respectively. The distributions of the SS, parameter b, apparent speed and apparent direction of movement for the identified irradiance transitions have been presented in Lappalainen and Valkealahti (2016a). The average length of the identified irradiance transitions calculated from b and the apparent speed was 116 m. The duration of the identified irradiance transitions calculated from the values of b varied from 0.96 to 420 s. The analyses of the apparent velocity and length of the identified irradiance transitions have been presented in Lappalainen and Valkealahti (2016b). For the studied PV arrays, a shading situation caused by an overpassing irradiance fall is symmetrical to a situation caused by a similar overpassing irradiance rise. Thus, the absolute values of parameter b for the identified irradiance transitions were used in the simulations.

In the identification of irradiance transitions, the 40% limit of minimum acknowledged SS was used because it has been shown by Lappalainen and Valkealahti (2015) that moving shadows with lower SS have no significant effect on the operation of PV strings. It has been shown in Lappalainen and Valkealahti (2016b) that the SS has no correlation with the duration, apparent speed or apparent direction of movement of irradiance transitions. Thus, the exact value of the applied minimum limit of SS has no significant effect on the shapes of the distributions of these characteristics or of the length of the irradiance transitions.

The simulations were conducted using time steps of 0.1 s and the irradiance at the centre of each PV module with an accuracy of 0.1 W/m^2 was used as the irradiance of that module during a time step. In the simulations, a shadow edge was assumed to be linear across a PV array and the apparent velocity of the shadow edge was assumed to be constant. A simulation period started when a linear shadow edge moved

Table 4
The average duration of the simulation periods for various areas.

Area	Duration (s)
Point	15.16
6 × 28 modules	21.46
8 × 21 modules	20.89
12 × 14 modules	20.94

over the first module of the PV array and ended when the shadow edge had moved across the array, i.e., when all the modules of the array were again uniformly shaded. To simplify the computation, the PV array was chosen to be under the constant STC irradiance of 1000 W/m^2 before each irradiance fall and the temperature of the PV modules was chosen as the constant STC temperature of 25 °C. During fast irradiance transitions, the changes in PV module temperatures are small having only a negligible effect on the operation of the modules. The length of the simulation periods varied from 2.5 to 1038 s, depending on the characteristics of the shadow edge and the dimensions of the PV array. The average duration of the simulation periods (irradiance transitions) is presented for various areas in Table 4.

The mismatch losses of a PV array were calculated as the difference between the sum of the global MPP powers of the PV modules of the array, as if the modules were operating separately, and the global MPP power of the array. Relative mismatch losses were calculated with respect to the sum of the global MPP powers of the PV modules.

3. Mismatch losses during the identified irradiance transitions

An example of the mismatch losses and the irradiance and output power fluctuations during PS caused by the movement of a cloud shadow edge over a PV array is offered in Fig. 2. The shading strength of the shadow edge was 85%, b 0.97 s, apparent speed 4.4 m/s and the apparent direction of movement 10° from the direction parallel to the PV strings of the array. As can be seen from Fig. 2, the PV output power decreases steeper than the irradiance does. The difference between the irradiance and output power fluctuations resulted mostly from the mismatch losses, as demonstrated by the combined curve of the mismatch losses and output power. The combined power curve is only slightly below the irradiance curve. The remaining small difference is caused by the fact that the relative output power of a PV module decreases faster than the relative irradiance received by the module when that irradiance is lower than the STC irradiance.

Mismatch losses during all the identified irradiance transitions were studied by using the curve fits of Eq. (2). The relative mismatch losses during all the identified irradiance transitions, the largest relative mismatch losses during a single irradiance transition and the largest instantaneous relative mismatch losses during the identified transitions for 6 × 28, 8 × 21 and 12 × 14 PV module arrays with SP, TCT and MS electrical configurations and a typical east-west orientation are presented in Table 5. The relative mismatch losses during all the identified transitions were the largest, about 4%, for the 6 × 28 SP array, and they decreased with decreasing string length. The differences between the electrical array configurations were small. However, the mismatch losses were the largest for the SP configuration. With string lengths of 28 and 21 PV modules, the mismatch losses of the TCT configuration were smaller than were those of the MS configuration, while with the string length of 14 modules the mismatch losses behaved oppositely. The behavior of the relative mismatch losses was in line with the findings of Lappalainen and Valkealahti (2017b). The largest relative mismatch losses during a single irradiance transition and the largest instantaneous relative mismatch losses were over 23% and 60%, respectively, for the 6 × 28 array layout with the SP configuration. Both of these maximum mismatch losses decreased only slightly with a changing array layout or electrical configuration. In addition to actual mismatch losses during the irradiance transitions, a mismatch of PV modules increases the transition rates of the PV output power with respect to the initial irradiance transition rates (Fig. 2).

Table 5
Relative mismatch losses of the studied PV arrays during all the identified irradiance transitions.

Electrical configuration	Layout	Relative mismatch losses (%)	Largest relative mismatch losses during an irradiance transition (%)	Largest instantaneous relative mismatch losses (%)
SP	6 × 28	4.04	23.7	61.1
SP	8 × 21	2.86	21.9	58.7
SP	12 × 14	1.63	21.6	53.5
TCT	6 × 28	3.92	23.7	60.6
TCT	8 × 21	2.69	21.0	58.1
TCT	12 × 14	1.40	21.4	53.3
MS	6 × 28	3.87	19.7	58.0
MS	8 × 21	2.68	19.3	56.6
MS	12 × 14	1.48	17.9	52.5

Because of the minor differences between the studied electrical PV array configurations, only the SP configuration is considered in the rest of this paper. The SP configuration was selected since it has generally the largest mismatch losses, and it is most commonly applied in real PV systems.

The relative cumulative frequencies of the relative mismatch losses for the three array layouts of the SP configuration during all the identified irradiance transitions are presented in Fig. 3. The relative mismatch losses were most of the time small, although large mismatch

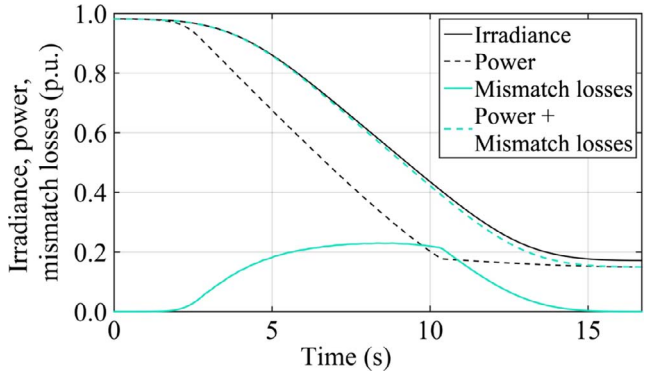

Fig. 2. Average irradiance, output power and mismatch losses for the 6 × 28 PV array layout with the SP configuration during partial shading caused by the movement of a shadow edge over the array. Irradiance is with respect to 1000 W/m^2 and power and mismatch losses to the nominal power of the array.

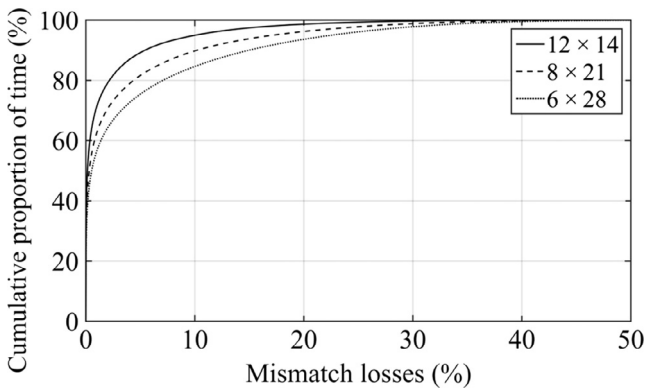

Fig. 3. Relative cumulative frequencies of the relative mismatch losses for the three array layouts of the SP configuration during all the identified irradiance transitions.

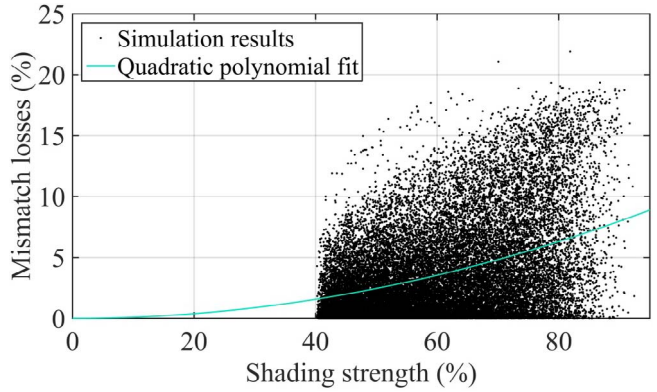

Fig. 4. Scatter plot between the mismatch losses of the 8 × 21 array layout with the SP configuration and the SS of all the identified irradiance transitions and a curve fit to the data.

losses also took place, but seldom. Half of the time of the transitions the relative mismatch losses of the 12 × 14, 8 × 21 and 6 × 28 SP arrays were less than 0.15%, 0.31% and 0.54%, respectively, and 80% of time they were less than 2.2%, 4.4% and 7.1%, respectively. The mismatch losses increased clearly with the increasing length of the PV array strings, thus in agreement with Table 5, and only a fraction of the irradiance transitions caused major mismatch losses. Those transitions had typically a high SS and a short length.

The scatter plot between the mismatch losses of the 8 × 21 SP array and the SS for all the identified irradiance transitions is presented in Fig. 4. Moreover, a quadratic polynomial fit with the simulation results is presented. It is good to notice that the 40% limit of minimum acknowledged SS was used in the identification of the irradiance transitions. These results show that the median, upper limit and dispersion of the mismatch losses increased with an increasing SS. The relative mismatch losses of over 19% were always caused by dark clouds leading to SSs above 70%. However, these shadows are quite rare, and clouds with higher transparency occur more often. The polynomial fit to the simulation results demonstrates how the typical mismatch losses decrease rapidly towards 0% when SS decreases below the 40% limit. This result suggests that weak shading transitions caused by moving clouds do not cause mismatch losses of any major general importance.

4. Total mismatch losses from moving clouds

The total mismatch losses of PV plants caused by moving clouds can be estimated based on the results of Section 3 and irradiance measurements. In doing so, the method presented by Lappalainen and Valkealahti (2015) was applied to identify all the irradiance transitions with SS over 5% during which the moving irradiance average of five seconds changed more than 1.5 W/m^2/s. With these lower limits of transition characteristics, all irradiance transitions should be considered with some practically meaningful mismatch losses. In total, 189,282 irradiance transitions were identified in the same measurement data of irradiance sensor S5 as earlier. The relative number of the identified irradiance transitions is presented in Fig. 5a as a function of the lower limit of acknowledged SS. The proportion of the irradiance transitions with more than 40% SS was about 23% of all the identified transitions, meaning that clouds cause mostly weak shadings with small SSs. The proportion of the time taken by all the identified irradiance transitions is presented as a function of the lower limit of acknowledged SS in Fig. 5b. The total duration of irradiance transitions with a SS over 5% was about 6% of the time, i.e., about 1.4 h in a day. This is a considerable share of the power production time for PV arrays.

The mismatch losses caused by all the 189,282 identified irradiance transitions were estimated using the following procedure. The relative mismatch power losses corresponding to the SS value of each transition

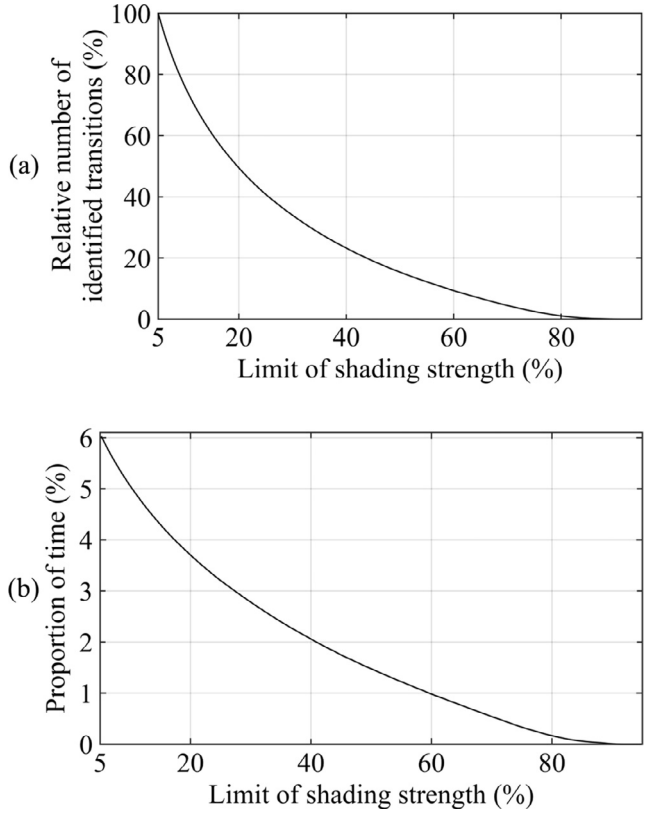

Fig. 5. Relative number of the identified irradiance transitions (a) and the proportion of the time taken by all the identified irradiance transitions (b) as a function of the lower limit of acknowledged SS.

were obtained from the fit of Fig. 4 for the 8 × 21 SP array layout and multiplied by the energy produced by the PV array during the PS as if the PV modules were operating separately. Mismatch losses for the 6 × 28 and 12 × 14 SP array layouts were calculated accordingly. The energy produced during the PS was calculated for a single PV module using the irradiance data measured with a sampling frequency of 10 Hz, and then was scaled for the PV array by the number of PV modules in the array and by using the average durations of the simulation periods as presented in Table 4. The energy production during the 15-month period was calculated similarly to the energy productions during the PSs by using the measured irradiance data with a sampling frequency of 1 Hz. Finally, the total relative mismatch losses caused by moving clouds were calculated by dividing the sum of the mismatch losses during the PSs by the total energy production for 15 months.

The relative total mismatch losses of the 6 × 28, 8 × 21 and 12 × 14 SP arrays are presented as a function of the lower limit of SS of the identified transitions in Fig. 6. The relative mismatch losses decreased more than linearly with the decreasing string length in accord with Lappalainen and Valkealahti (2017a). In total, almost 80% of the total mismatch losses were caused by the irradiance transitions of over 40% SS although the proportion of these transitions was only a little over 20% of the analysed 189,282 transitions (see Fig. 5a). This result supports the selection of the 40% limit of minimum acknowledged SS used in the identification of irradiance transitions.

As can be seen from Fig. 6, the relative mismatch losses level off with the decreasing limit of SS at small values, indicating that the chosen 5% lower limit is small enough for the presented study. The results show that the total mismatch losses of the 6 × 28, 8 × 21 and 12 × 14 PV arrays caused by moving clouds were about 0.48%, 0.35% and 0.21%, respectively. These results are in line with the estimation presented in Lappalainen and Valkealahti (2017b), namely, that the mismatch losses caused by moving clouds are clearly below 1.0% of the

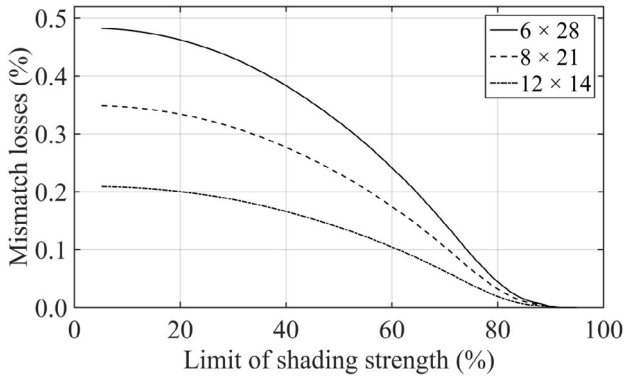

Fig. 6. Relative mismatch losses of the three PV array layouts of the SP configuration during all the identified irradiance transitions as a function of the lower limit of acknowledged SS.

total electricity production of PV arrays. In total, the mismatch losses caused by moving clouds do not seem to be a major problem for PV power production. However, minor improvement in energy production can be achieved by minimizing the maximum diameter of PV module strings.

The distribution of the total mismatch losses as a function of the SS of the irradiance transitions is presented in Fig. 7. The distribution is the same for all the three studied PV array layouts. The proportion of the mismatch losses caused by the shadow edges of the clouds with high transparency (SS less than 20%) was small even though the share of these transitions was roughly half of all the transitions (Fig. 5a). The reason for this is that these shadow edges cause only minor mismatch losses (Fig. 4). For the irradiance transitions with very high SSs, the situation was opposite; the mismatch losses during these transitions can be large but these transitions are very rare. Thus, the proportion of the mismatch losses caused by the shadow edges of extremely dark clouds was also small. Most of the mismatch losses, about 70%, were caused by the shadow edges with SSs between 40% and 80%. These shadow edges have high enough SSs to cause major mismatch losses, and they are frequent enough to have a high cumulative effect.

5. Discussion

In this study, especially in the estimation of the overall effect of the mismatch losses caused by moving clouds, several assumptions were made. In the method to define the apparent velocities of the identified shadow edges presented by Lappalainen and Valkealahti (2016b), the following three assumptions were used: the apparent velocity of the shadow edge while passing over the used sensor triplet is constant, the shadow edge is linear across the irradiance sensor array and the shadow covers all the three sensors. These assumptions are generally satisfied

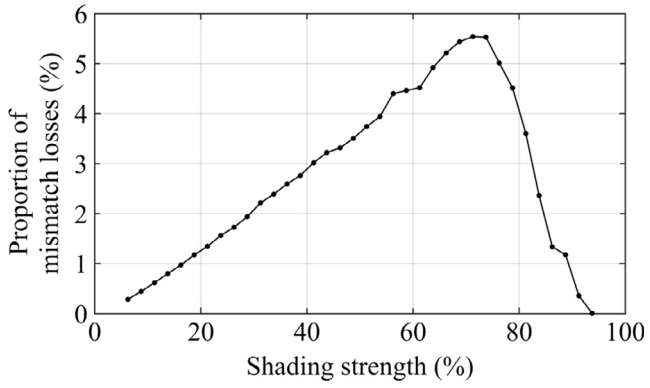

Fig. 7. Proportion of total mismatch losses caused by irradiance transitions with different SSs.

for closely placed sensors, but the results are used for the whole PV array in this study. However, the maximum dimension of about 40 m of the studied PV arrays (see Table 3) is not drastically larger than the dimensions of the sensor array. Therefore, the cloud shadow edges can be assumed to be nearly linear for the whole array area, and the changes in their apparent velocity while passing over the array can be expected to be small. Moreover, Lappalainen and Valkealahti (2017a) have found that the mismatch losses are sensitive to the variation of the apparent speed only at small speeds. Thus, these assumptions of the linearity and constant apparent velocity of shadow edges should not have caused significant errors to the presented results.

In the estimation of the overall effect of the mismatch losses, irradiance transitions identified in single point measurements were used, and it was assumed that the shadows covered the whole PV array. For the PV array, the number of irradiance transitions can be larger than for a single point since the PV array detects irradiance fluctuations on a larger area than a point sensor. However, the point sensor measurement describes the irradiance at the centre of the PV array and irradiance transitions taking place only on the border of the array will shade the whole array marginally like the transitions with SS smaller than 5% (see Fig. 6). The conclusion is that the use of the single point irradiance measurements did not cause major errors to the results.

In the simulations, only the time when the PV array is becoming shaded or unshaded, i.e., when a shadow edge is moving over the array, was studied. However, the irradiance during a clear sky or overcast situation is never perfectly even, i.e., there are always minor differences in the irradiance levels received by the PV modules. Thus, some mismatch losses also exist when the identified transitions are not taking place. However, the differences in irradiance levels between the modules in those situations are very small. As presented in Fig. 4, small SS leads to minor mismatch losses. Thus, the mismatch losses caused by moving clouds when the whole array is shaded or during clear sky conditions can be regarded as negligible.

The temperature of all the PV modules was assumed to be the same in the simulations. In reality, irradiance differences cause temperature differences and mismatches between the modules. Moreover, mismatch losses caused by temperature differences also occur whether the whole array is shaded or unshaded. However, the thermal mass of the PV modules is so high and the irradiance transitions are mostly so fast that the module temperatures do not change considerably during most of the irradiance transitions. During the longest transitions, temperature changes may be considerable. However, in these cases, irradiance differences between the modules are small, thus leading to only small temperature differences.

In conclusion, several assumptions were made in this study, and the total mismatch losses of PV power plants caused by moving clouds might be somewhat larger than are presented in this paper. However, it is clearly evident that the total mismatch losses of PV arrays caused by moving cloud shadows are very small. Since PV arrays are the operational units of large PV power plants, this result is valid for larger PV power plants as well.

It is also good to note that only the mismatch losses caused by moving clouds were studied in this study, and there are other sources of mismatch losses. Sharp shadows caused by nearby objects can lead to significantly larger mismatch losses and to larger differences between the electrical PV array configurations (Lappalainen and Valkealahti, 2017a). Moreover, mismatch losses caused by manufacturing tolerances exist in every PV system. The soiling and damage of PV modules can also cause mismatch losses. Thus, the total mismatch losses of PV systems might be substantially larger than the mismatch losses caused by moving clouds. In addition to the mismatch losses, overpassing cloud shadows will cause losses through failures in MPP tracking. MPP tracking losses depend largely on the used MPP tracking algorithm and might momentarily be much higher than the mismatch losses. Thus, although the total mismatch losses caused by moving clouds are small, the total losses caused by moving clouds might be considerable.

Moreover, cloud shadows cause fast irradiance transitions leading to fluctuations in the output power of PV systems, which can lead to power quality problems and grid stability issues.

6. Conclusions

In this paper, the mismatch losses of SP, TCT and MS electrical PV array configurations and various array layouts during about 27,000 irradiance transitions identified in measured irradiance data for 15 months were studied. Moreover, the total mismatch losses of PV plants caused by moving clouds were determined based on around 190,000 irradiance transitions identified in the measured data. The study was conducted using a mathematical model of irradiance transitions and an experimentally verified MATLAB/Simulink model of a PV module.

The relative mismatch losses during the identified irradiance transitions ranged from 1.4% to 4.0% depending on the electrical configuration and layout of the PV array. Most of the time during the transitions, the relative mismatch losses were less than 1%, while large mismatch losses seldom took place. The largest observed instantaneous relative mismatch losses were over 60%. The differences between the electrical PV array configurations were small, and the mismatch losses decreased with a decreasing PV string length in accord with previous studies.

The overall effect of the mismatch losses caused by moving clouds on the electricity production was about 0.5% for the PV array with strings of 28 PV modules and substantially smaller for the arrays with shorter strings. The proportions of the mismatch losses caused by the shadow edges of very dark clouds or clouds with high transparency were small. About 70% of the total mismatch losses were caused by the shadow edges having shading strengths between 40% and 80%. In total, the mismatch losses caused by moving clouds do not seem to be a major problem for the energy production of large-scale PV plants. However, minor improvement in energy production can be achieved by minimizing the maximum diameter of PV module strings.

Sharp shadows, caused by nearby objects, can lead to significantly larger mismatch losses than the shadows of moving clouds. Moreover, the manufacturing tolerances, damages and uneven soiling of PV modules can also cause mismatch losses. Thus, the total mismatch losses of PV systems may be substantially larger than the mismatch losses caused by moving clouds. In addition to mismatch losses, overpassing cloud shadows can also cause MPP tracking losses and output power fluctuations.

References

Lappalainen, K., Valkealahti, S., 2015. Recognition and modelling of irradiance transitions caused by moving clouds. Sol. Energy 112, 55–67.

Lappalainen, K., Valkealahti, S., 2016a. Mathematical parametrisation of irradiance transitions caused by moving clouds for PV system analysis. In: Proceedings of 32nd European Photovoltaic Solar Energy Conference, pp. 1485–1489.

Lappalainen, K., Valkealahti, S., 2016b. Apparent velocity of shadow edges caused by moving clouds. Sol. Energy 138, 47–52.

Lappalainen, K., Valkealahti, S., 2017a. Effects of irradiance transition characteristics on the mismatch losses of different PV array configurations. IET Renew. Power Gener. http://dx.doi.org/10.1049/iet-rpg.2016.0590.

Lappalainen, K., Valkealahti, S., 2017b. Effects of PV array layout, electrical configuration and geographic orientation on mismatch losses caused by moving clouds. Sol. Energy 144, 548–555.

Lave, M., Reno, M.J., Broderick, R.J., 2015. Characterizing local high-frequency solar variability and its impact to distribution studies. Sol. Energy 118, 327–337.

Lorente, D.G., Pedrazzi, S., Zini, G., Dalla Rosa, A., Tartarini, P., 2014. Mismatch losses in PV power plants. Sol. Energy 100, 42–49.

Perez, R., Kivalov, S., Schlemmer, J., Hemker, K., Hoff, T., 2011. Parameterization of site-specific short-term irradiance variability. Sol. Energy 85, 1343–1353.

Picault, D., Raison, B., Bacha, S., de la Casa, J., Aguilera, J., 2010. Forecasting photovoltaic array power production subject to mismatch losses. Sol. Energy 84, 1301–1309.

Potnuru, S.R., Pattabiraman, D., Ganesan, S.I., Chilakapati, N., 2015. Positioning of PV panels for reduction in line losses and mismatch losses in PV array. Renewable Energy 78, 264–275.

Rakesh, N., Madhavaram, T.V., 2016. Performance enhancement of partially shaded solar PV array using novel shade dispersion technique. Front. Energy 10, 227–239.

Rodrigo, P., Velázquez, R., Fernández, E.F., Almonacid, F., Pérez-Higueras, P.J., 2016. Analysis of electrical mismatches in high-concentrator photovoltaic power plants with distributed inverter configurations. Energy 107, 374–387.

Shams El-Dein, M.Z., Kazerani, M., Salama, M.M.A., 2013a. An optimal total cross tied interconnection for reducing mismatch losses in photovoltaic arrays. IEEE Trans. Sustain. Energy 4, 99–107.

Shams El-Dein, M.Z., Kazerani, M., Salama, M.M.A., 2013b. Optimal photovoltaic array reconfiguration to reduce partial shading losses. IEEE Trans. Sustain. Energy 4, 145–153.

Tomson, T., 2010. Fast dynamic processes of solar radiation. Sol. Energy 84, 318–323.

Tomson, T., Tamm, G., 2006. Short-term variability of solar radiation. Sol. Energy 80, 600–606.

Torres Lobera, D., Valkealahti, S., 2013. Mismatch losses in PV power generators caused by partial shading due to clouds. In: Proceedings of 4th IEEE International Symposium on Power Electronics for Distributed Generation Systems.

Torres Lobera, D., Mäki, A., Huusari, J., Lappalainen, K., Suntio, T., Valkealahti, S., 2013. Operation of TUT solar PV power station research plant under partial shading caused by snow and buildings. Int. J. Photoenergy 2013, Article ID 837310.

Vijayalekshmy, S., Bindu, G.R., Rama Iyer, S., 2016. A novel Zig-Zag scheme for power enhancement of partially shaded solar arrays. Sol. Energy 135, 92–102.

Villa, L.F.L., Picault, D., Raison, B., Bacha, S., Labonne, A., 2012. Maximizing the power output of partially shaded photovoltaic plants through optimization of the interconnections among its modules. IEEE J. Photovoltaics 2, 154–163.

Villalva, M.G., Gazoli, J.R., Filho, E.R., 2009. Comprehensive approach to modeling and simulation of photovoltaic arrays. IEEE Trans. Power Electron. 24, 1198–1208.

Wenham, S.R., Green, M.A., Watt, M.E., Corkish, R., 2007. Applied Photovoltaics, second ed. Earthscan, London.